Redox Conditions of Late Neoproterozoic and Early Cambrian *Lagerstätten*

Andrew Doerrler

Department of Geology, University of Maryland, College Park

GEOL 394

Dr. Alan Jay Kaufman

April 25, 2023

Scientific Abstract

Shale samples from two fossiliferous localities in the Russian Federation, including the Fortunian Stage (Cambrian Period) Chuskuna Formation in the Olenek Uplift south of the Lena Delta in arctic Siberia, and the Ediacaran Period Zimnie Gory and Erga in the White Sea region of Fennoscandia have been acquired. The Chuskuna Formation, which is 20 million years older than the Burgess Shale, contains a remarkable Lagerstätten (deposit that exhibits extraordinary fossils with exceptional preservation) of organic tissues representing as many as 10 separate animal phyla, while the Zimnie Gory and Erga formations contain exceptionally preserved impressions of Ediacaran biota of the globally distributed White Sea assemblage. The hypothesis is that anoxia in the sediments/water column led to the exceptional preservation of the fossils in both the Ediacaran and Fortunian examples from the Russian Federation. To understand the redox conditions that allowed for exceptional preservation of fossils, sample powders were prepared for acidification to determine the % carbonate and for leaching to determine iron abundance of carbonate, oxide, magnetite, and silicate fractions, respectively. Yields of sulfur in the form of Ag_2S from CRS (chrome reducible sulfur) extraction provided the iron abundance of the sulfide fraction of samples. Thallium isotope measurements were collected to serve as an additional redox proxy. These data serve as a proxy for local redox conditions (oxic, suboxic, anoxic, or euxinic) of the sediments and water column at the time of shale accumulation and early diagenesis. Iron speciation reveals low levels of iron in the measured phases. The measured iron in the silicate phases is high, however it is not enough to account for all of the iron in the sediments, suggesting that majority of the iron is detrital. Observations of glauconite in thin sections of the shales support anoxic or dysoxic conditions in sedimentary pore waters. However, there is no discernible metal enrichment that would be expected with anoxic/euxinic conditions. This is inconsistent with the expectation that the sediments would likely need to be anoxic to preserve the fossil remains and impressions but may be the result of: 1) ferruginous rather than sulfidic conditions; or, 2) the long-term depletion of metals from the oceanic inventory.

Plain Text Summary

While the preservation of animal shells and bones is relatively common, organic remains of animal soft parts preserved in ancient sedimentary rocks are rare. Soft tissue preservation provides unique windows into past environments and ecology, especially in the Ediacaran and Cambrian periods when animals first evolved This study aimed to understand the environmental conditions in which soft tissues associated with the mysterious Ediacaran biota and the oldest known Cambrian Burgess Shale-type biota of the Russian Federation, were preserved. In particular, we evaluated the iron concentration in carbonates, oxides, sulfides, and silicate minerals in shale samples to reconstruct the oxidation state of fine-grained sediments in which these fossils were preserved. Based on iron abundance data, the depositional conditions in both examples were lacking in oxygen, which were supported by thin section observations, total element abundances, and thallium isotope signatures for the Cambrian example. In summary, the geochemical measures support the view that a lack of oxygen promoted the preservation of organic tissues, and that many of the early animals may have been tolerant of low oxygen conditions.

Introduction

Characterization of the depositional environment of shale samples from two fossiliferous localities in the Russian Federation (Fig. 1). The two localities are the Fortunian Stage (Cambrian Period) Chuskuna Formation (Grazhdankin et al., 2020) in the Olenek Uplift south of the Lena Delta from arctic Siberia, and the Ediacaran Period Zimnie Gory and Erga formations (Martin et al., 2000) in the White Sea region of Fennoscandia. These shale horizons contain exceptionally well-preserved organic walled tissues related to as many as 10 different animal phyla (Fig. 2a), as well as imprints of soft-bodied Ediacaran biotas (Fig. 2b) in unconsolidated shaley lithofacies, respectively.

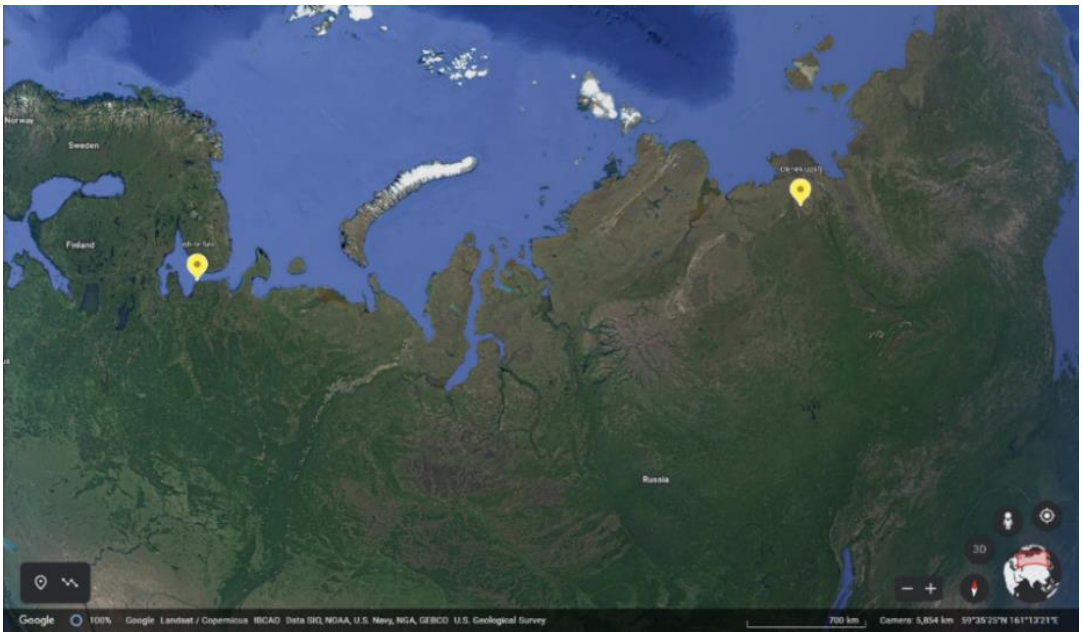

Figure 1: White Sea (Left) and Olenek Uplift (Right) (Google Earth Pro)

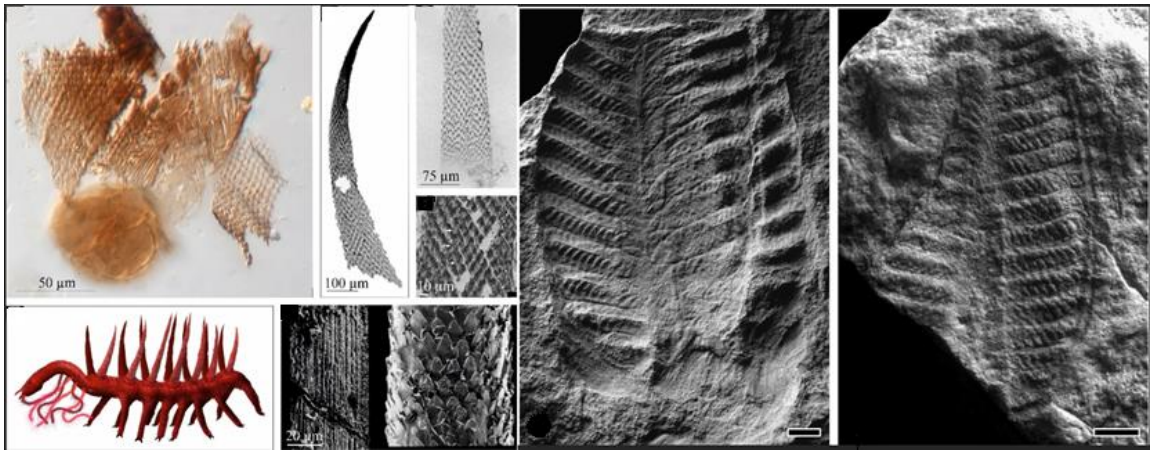

Figure 2a: Cuticular aggregation and similar ornamentation from earlier findings. Cuticular aggregation with distinctive microstructure. Provided by Olga Dantes

Figure 2b: Rangea., PIN 3993-7021; collected in sandstone-filled overflow channels of the distributary-mouth bar setting, Erga Fm. (Modified from Grazhdankin, 2004)

The fauna of the Ediacaran Period is divided into three different groups called assemblages, which reflect systematic biological turnover or environmental, taphonomic or biogeographic biases. The three assemblages are the Avalon (570-560 Ma), the White Sea (560-550 Ma), and the Nama assemblages (550-541 Ma) (Fig. 3; Droser et al., 2017). The Zimnie Gory and Erga formations serve as key localities for the fauna of the White Sea assemblage. The exceptional preservation of the soft-bodies Ediacaran biotas as carbonaceous compression (Bobrovsky et al., 2018) in the shaley lithofacies is made even more extraordinary by the rather unconsolidated nature of the formation. The shale of the Zimnie Gory and Erga formations has most impressions preserved in fine to medium-grained sandstones, so this mudstone is mostly remarkable for being 550 million years old and hardly consolidated.

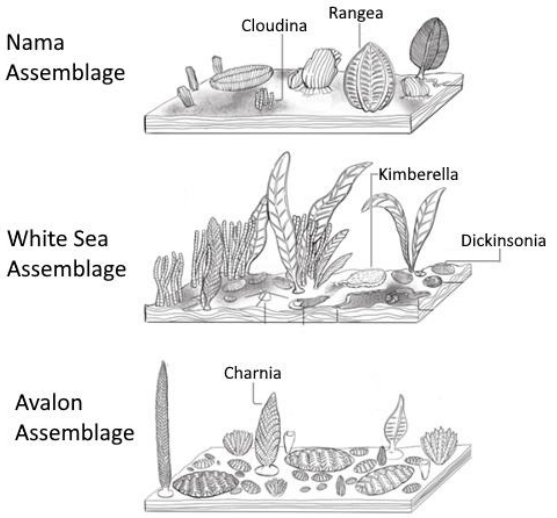

Figure 3: Illustration of the three Ediacaran assemblages. (Modified from Droser et al., 2017).

The organic tissues of the Chuskuna Formation provide the oldest fossil evidence for fauna commonly associated with the world-famous Burgess Shale. The Chuskuna Formation is constrained by the 529.7 Ma age of an underlying volcanic ash in the Mattaia Formation (Fig. 4; Grazhdankin et al., 2020), which constrains the biota to be 10 million years older than the fossiliferous Chengjiang Formation (Hou et al., 1991), and over 20 Ma older than the Burgess Shale (Walcott, 1912; Butterfield, 2003). This discovery implies that the Cambrian explosion happened much faster than previously thought.

The added complication of diagenesis and other post depositional processes is something to consider when attempting to characterize the depositional environment. As is the nature of shale, it is porous, but highly impermeable, meaning that hydrothermal alteration after deposition would not have a major impact. While hydrothermal alteration causing fractures or brecciation in shale is certainly possible, it is unlikely to have occurred in these formations as those features are not seen. For the samples in this paper, the rock units display no evidence metamorphic alteration. In fact, the shale

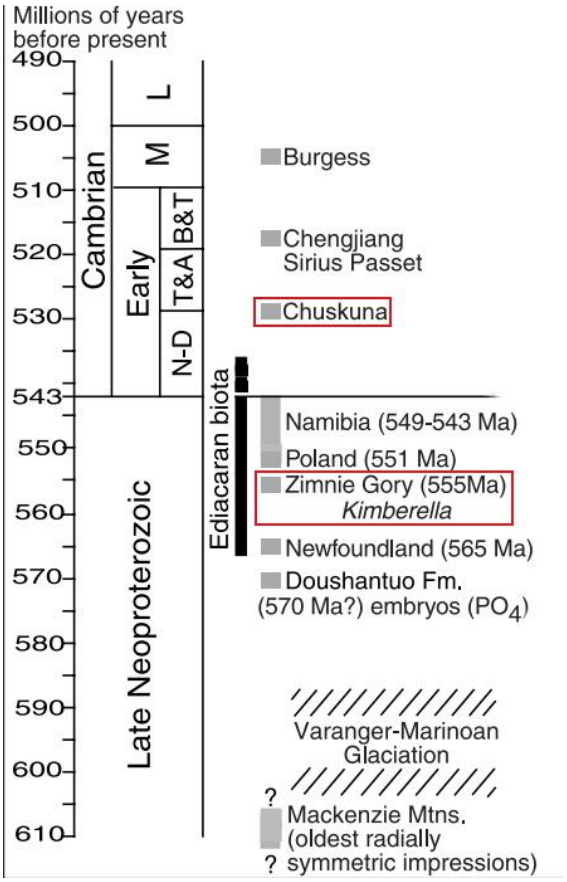

Figure 4: Geologic time scale relating the Zimnie Gory and Chuskuna Formations. (Modified from Martin et al., 2000)

of the Zimnie Gory and Erga formations are so poorly consolidated it is astounding that that the rocks are 550 million years old, and still contain such exceptional fossils. Many redox-sensitive elements are tightly bound to reduced phases, such as organic matter and sulfides in the rock, making them more difficult to alter than elements that are contained in other phases, like a carbonate crystal lattice. Under reducing conditions redox-sensitive metals are highly insoluble and would remain in solid phases, resulting there being little impact by burial diagenesis.

Hypothesis

The exceptional preservation of the body and trace fossils in the Chuskuna, Zimnie Gory, and Erga formations is yet to be fully understood. The mode of fossil preservation suggests that there was either little free oxygen in the water column, or that there was a rapid depositional event, resulting in the burial of the organisms. Both of these conditions are likely for the Chuskuna since many of the fossil fragments appear to be transported rather than in situ. If the organisms lived in oxic environments, this transportation could have moved them to a anoxic environment. The Zimnie Gory and Erga organisms may have lived beneath algal mats, indicating a lack of oxygen, but otherwise are not likely to have been transported very far between time of death and time of burial. The hypothesis is that anoxia in the sediments/water column led to the exceptional preservation of the fossils in both the Ediacaran and Fortunian examples from the Russian Federation. The null hypothesis is that there is no anoxia in the sediments/water column, so the exceptional preservation was due to other processes.

Geology

The White Sea Region

The Zimnie Gory Formation (Ediacaran Period) is located in the White Sea region on the northwest coast of Russian Fennoscandia. It is approximately 60 meters thick, comprises poorly consolidated laminated shale, interstratified sandstone, and alternating shale, siltstone, and sandstone (Fig. 5). The studied interval represents 10 meters of laminated shale, which is in the contact

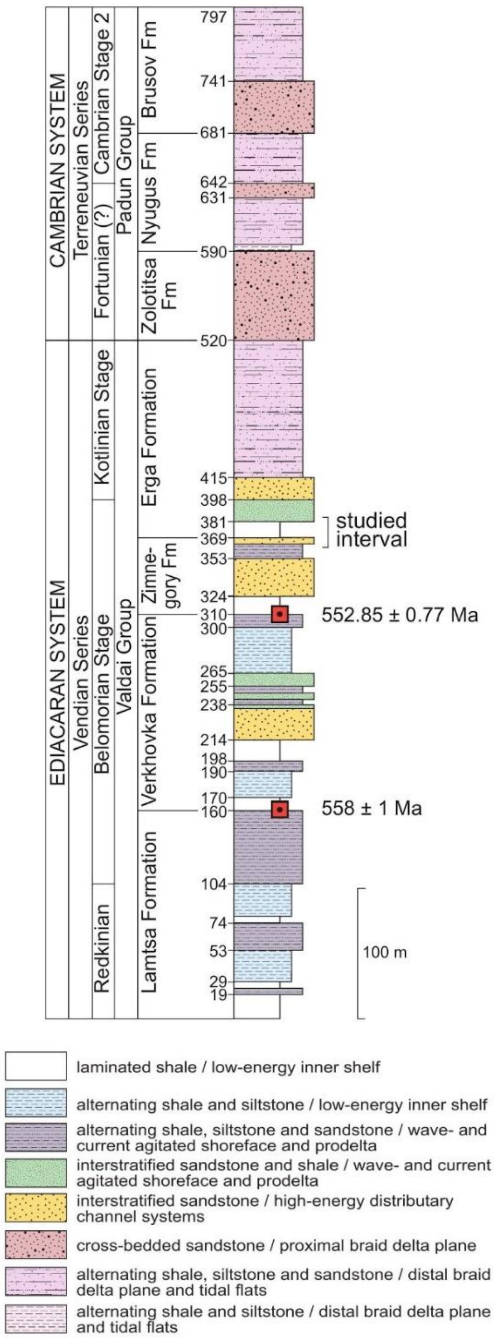

Figure 5: (Right) Stratigraphic and key of the White Sea region.

Courtesy of Dimitry Grazhdankin

between the top of the Zimnie Gory Formation and base of the Erga Formation. The depositional environment is interpreted to be estuarine, with signs of a gradual progradation, from a submarine valley to a prodelta setting (Grazhdankin, 2003). The age of the Zimnie Gory is constrained by zircons within a volcanic ash layer, beneath the fossiliferous beds, to 555.3 Ma (Martin et al., 2000), which provides an important temporal constraint for the White Sea biota. The Erga formation lies directly above the Zimnie Gory Formation. It is approximately 150 meters thick. The lowest 50 meters are comprised of laminated shale and interstratified sandstone and shale. The upper 100 meters is characterized by alternating shale, siltstone, and sandstone. The depositional environment of the Erga Formation is interpreted to be a marine prodelta lithofacies, which implies a transgressive sequence (Grazhdankin, 2003). A total of 26 samples were collected from the Zimnie Gory and Erga formations. The interval where they were collected is the white layer on the stratigraphic column, at the boundary between the Zimnie Gory and Erga formations (Fig. 5).

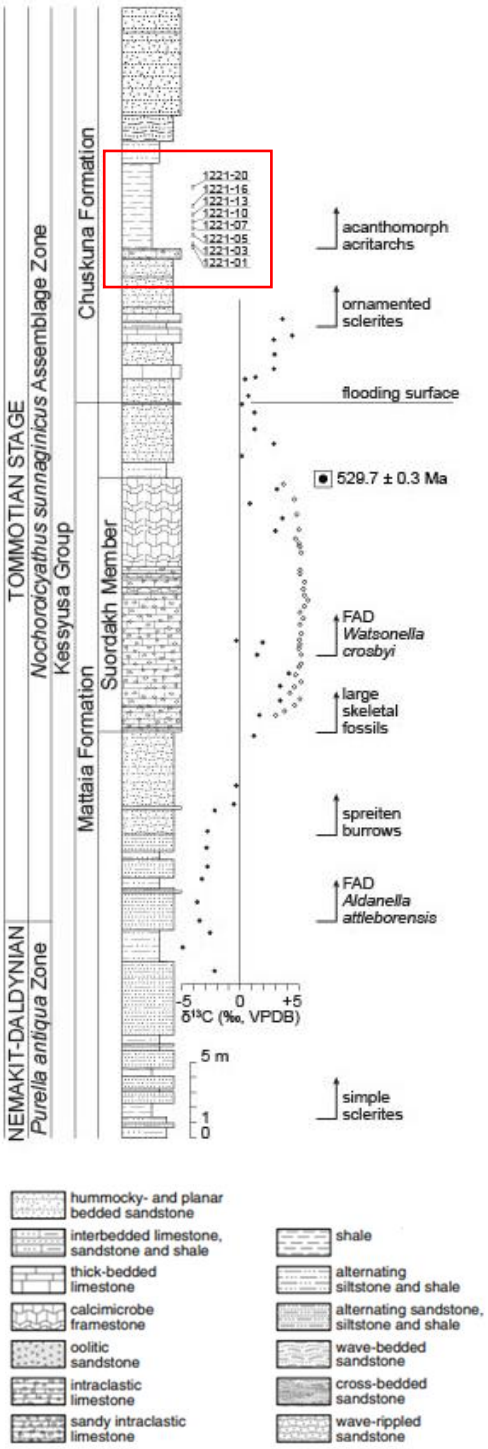

Figure 6: (Left) Stratigraphic Column of the Olenek Uplift. The red box indicates the sampling area.

(Modified from Grazhdankin et al., 2020)

The Chuskuna Formation

The Chuskuna Formation (Fortunian Stage of the Cambrian Period) is located in the Olenek Uplift south of the Lena Delta, in arctic Siberia. The Chuskuna Formation is approximately 26 meters thick and is composed of a depositional parasequence bounded by flooding surfaces. The base of the formation is a transgressive sequence of intensely bioturbated sandstone followed by interstratified limestone, shale, and conglomerate. The transgressive deposit underlies laminated shale, with fine-grained sandstone. The sandstone coarsens upward into medium and coarse grained lithologies, some of which is intensely bioturbated in the upper layers (Fig. 6). The depositional sequence is capped by coarse-grained channelized sandstone, which is interpreted as a prodelta deposit (Grazhdankin et al., 2020). The prodelta interpretation for these formations could provide a mechanism for the burial of organic fragments. Prodelta deposits form at the mouth of deltas, where the sediments pile up, forming steep underwater slopes, and eventually spill over forming turbidities. As these underwater landslides occur, organisms living on the slopes get caught in the flow. This characteristic deposit, termed a Bouma sequence, is seen in the upper part of the Chuskuna Formation. Eight samples from the Chuskuna Formation were collected from the shale layer in the middle of the formation (Fig. 6).

Methods

Sample Preparation The initial sample preparation was done in order to perform each of the analyses (Fig 7). This preparation required the use of an MK Diamond Products Inc. rock saw to cut the samples down to a smaller size, to assist with the rest of the preparation procedures. It was important that throughout the preparation, the samples did not come in contact with any metal, as that would contaminate the data extracted from the iron speciation. A LaboPol-21 grinder/polisher with silicon carbide grinding pads was used to grind and polish the surfaces of the rocks that came into contact with the blade of the rock saw. This was performed in order to avoid iron contamination from the saw blade. The samples were then crushed into pea-sized pieces using a rock hammer, which was covered in plastic wrap in order to prevent the sample from coming into contact with metal. The crushed samples were then turned into a very fine powder (200 mesh) using a SPEX SamplePrep 8000M Mixer/Mill. In between samples, a cycle of the ball mill was run with annealed sand to prevent cross contamination of the samples. The sand was annealed by placing it a furnace at 500°C for two hours to remove organics to prevent the organic content in the sand from getting incorporated into the sample. The agate housing of the ball mill was cleaned in between each sample with ethanol and 1 M HCl as an additional measure to prevent cross contamination.

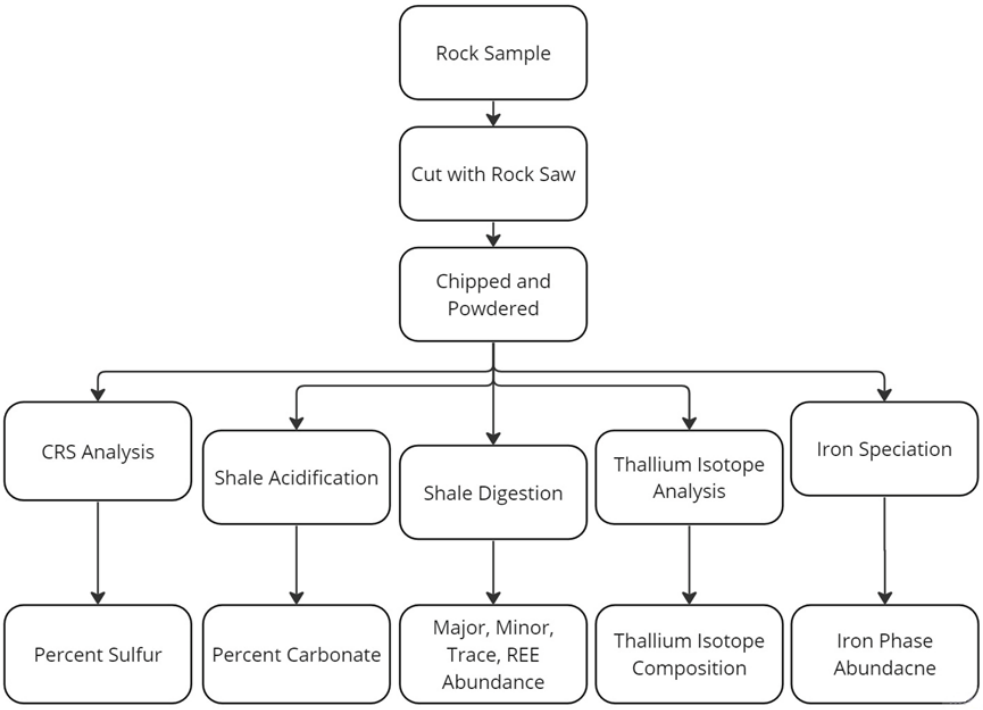

Figure 7: Flow diagram of the procedures completed and the type of result for each type of analysis.

With the powdered sample, chrome reducible sulfur (CRS) extractions were performed to obtain sulfur content, which is later used in iron speciation calculation. The powdered sample was also acidified and dissolved in order to obtain % carbonate and whole rock major, minor, trace, and rare earth element abundance data, respectively. Iron speciation was performed to quantify the redox conditions. Thallium isotopes were measured as another redox proxy.

CRS Extraction Chrome reducible sulfur (CRS) analysis was performed following a standard operating procedure written by Alan J. Kaufman, based on Canfield et al. (1986). This was accomplished using an aliquot of powdered sample to obtain sulfur content (which was later used in iron speciation calculations). The glassware used in this procedure was first cleaned in a 10% HCl bath and then rinsed with tap water and subsequently - 18 MΩ Milli-Q water. Approximately 100 mg of the powdered sample was weighed into labeled boiling flask inlets. Each boiling flask was attached with lower adaptors in heating mantles beneath the condensers. Blue rubber septa were placed into the arm of each flask, being screwed in to form a seal using black injection screws. Labeled glass tubing was placed into each of the six glass inlet ports on the lower adapters. A small volume of high vacuum grease was applied to the ground glass end of the upper adapter joints and attached to the top of the condenser. The water trap was filled with Milli-Q water to one cm below the ground glass interior. A small volume of high vacuum grease was applied to the ground glass and fit to on the upper adapter of the water trap. The water trap was attached to the upper adapter and then the blue Keck clips were attached to hold the taper fittings together. A small amount of high vacuum grease was applied to the glass joints of the tube adaptors and then those were attached to the upper adaptors. Labeled test tubes were placed into a test tube rack and filled with 25 mL of silver nitrate solution. The test tubes were then attached above the condensers using wooden clothes pins. Pasteur pipettes were attached to the rubber housing on the six tube adaptors. A short Pasteur pipette was attached to an N_2 hose and inserted into a beaker with 150 mL of 5 M HCl and covered with Parafilm. The chilled water re-circulator attached to the condensers was turned on. The N_2 tank was allowed to flow into the apparatus at a rate of one to two bubbles per second in the water trap. The system was checked for leaks before proceeding with the extraction. The nitrogen valve was opened to the CRS hood. A 20 mL Luer-Lok syringe was inserted into the CRS extraction port to draw up 20 mL of the solution. The solution was slowly injected through the blue rubber septa into the boiling flask and repeated for the remaining five flasks. The same syringe and needle were used to draw 20 mL aliquots of the degassed 5 M HCl and injected into each of the boiling flasks. The heating mantles beneath the boiling flasks were turned on to 120 V. The heating mantles were turned off after three hours. The labeled tubes were transferred to the test tube rack in the CRS fume hood, and then the water traps were disassembled, along with the upper and lower adapters. The CRS solution and sediment from the boiling flasks were properly disposed of. The disassembled parts of the apparatus and the boiling flasks were properly cleaned before the next set of samples. This process was repeated for all of the samples. The Ag_2S sample in $AgNO_3$ solution was separated and transferred to labelled two mL centrifuge tubes using disposable pipettes. The samples were then centrifuged in the Farquhar laboratory (CHEM 0230) at 10,000 rotations per minute, for three minutes in the micro-centrifuge. The supernatant was then pipetted into a waste beaker. The centrifuge tubes were placed on a hot plate at 70ºC for two hours to dry. The dried sample was then weighed to quantify the abundance of Ag_2S and to calculate the sulfur content of the extracted sample. The sulfur content was later used as part of the iron speciation calculations.

Shale Acidification In order to determine the % carbonate, a standard operating procedure developed by Geoff Gilleaudeau was followed. This was performed by weighing between one and two grams of each powdered sample which was placed into separate 50 mL centrifuge tubes. The samples were then dosed with separate rounds of 3M HCl and hot 6M HCl to remove the carbonate fraction. This carbonate fraction might include relatively insoluble iron-bearing carbonates such as siderite and ankerite (or ferroan dolomite). In between the addition of each acid, the samples were centrifuged at 5,000 rotations per minute for 10 minutes and decanted into a labelled waste

container before the next aliquot of acid was added. After the 6 M HCl was decanted, 20 ml of 18 MΩ Milli-Q water was added to the samples to neutralize the remaining solution. The samples with Milli-Q water were then centrifuged at 5,000 rotations per minute for 10 minutes and decanted. The samples were rinsed with Milli-Q water twice to ensure the samples were thoroughly neutralized. The samples were placed, uncapped, in a drying oven at 80°C overnight. The weight difference between the initial powdered samples and the acidified residues allowed for the quantification of % carbonate in each sample.

Shale Dissolution Total shale dissolution treatments were conducted following a standard operating procedure developed by Geoff Gilleaudeau. This was performed with an aliquot of powdered samples in order to obtain whole rock major, minor, trace, and rare earth element abundance data. The first step of shale digestion was to remove any organic material in the sample. This was done by placing approximately 120 mg of each sample into ceramic crucibles which were set in a muffle furnace at 550°C for six hours. The ashed samples were then placed into separate Teflon beakers. Five mL of concentrated trace-metal grade (TMG) HNO_3 and one mL of concentrated TMG HF was added to each beaker and left, capped, on a 180°C hotplate overnight. The beakers, still on the hotplate, were then uncapped to allow the solution to partially dry down. Once the solution was partially dried down the beakers were removed from the hotplate and allowed to cool completely. Once the beakers were cooled, two mL of concentrated TMG HCl were added to each beaker. They were capped and left on a 180°C hotplate overnight, followed by partially drying down the solution. The final solution of five mL of 6M TMG HCl and two drops of concentrated TMH HF were added to the beakers. The beakers were then capped and left on a hotplate set to 180°C overnight. Once the beakers cooled, 100 µL of the samples were added to separate 15 mL centrifuge tubes with 9.9 mL of two % TMG HNO_3. The solutions were sent off to Arizona State University for analyses to obtain major, minor, trace, and rare earth element abundance data using an ICP-MS. This was to better understand seawater redox, productivity, and salinity. The Relative Standard Deviation (RSD) of repeated measurements of an in-house standard check for each element is reported as analytical uncertainty in percent for each element (Appendix 1).

Iron Speciation Iron speciation was implemented by following a standard operating procedure developed by Geoff Gilleaudeau, to quantify the redox conditions. This was achieved through a series of three different leach solutions. The first leach solution was a sodium acetate (1 M sodium acetate [$C_2H_3NaO_2$] solution buffered with acetic acid [CH_3COOH] to pH 4.5**),** which extracted any iron associated with carbonate phases (siderite or ferroan dolomite). The second leach solution was sodium dithionite, (50 gL-1 sodium dithionite [$Na_2S_2O_4$] solution buffered with 0.35 M acetic acid [CH_3COOH] and 0.2M sodium citrate [$Na_3C_6H_5O_7 \cdot H_2O$] to pH 4.8), which extracted any iron associated with oxides (goethite or hematite). The third and final leach was ammonium oxalate, 0.2 M ammonium oxalate [$C_2H_8N_2O_4 \cdot H_2O$], 0.17 M oxalic acid [$H_2C_2O_4 \cdot 2H_2O$] solution buffered with ammonium hydroxide [NH_4OH] to pH 3.2), which extracted any iron associated with magnetite. Approximately 200 mg of powdered sample and 10 mL of the sodium acetate solution were put into sperate 15 mL centrifuge tubes. They were placed on a rotating rack for 48 hours. The tubes were then centrifuged at 5,000 rotations per minute for five minutes. The solution was then decanted into new 15 mL centrifuge tubes and set aside for later analysis. Ten mL of the sodium dithionite solution were then added to the centrifuge tubes containing the leached samples from the previous step. These samples were placed on a rotating rack for two hours. They were then centrifuged and decanted into new centrifuge tubes. Ten mL

of ammonium oxalate were added to the centrifuge tubes containing the leached sample from the previous step. These samples were placed on a rotation rack for six hours. They were then centrifuged, and the solution decanted into new centrifuge tubes. The leached powder from the White Sea was properly disposed of, while the leached powder from the Chuskuna Formation was used for one additional leach. The additional leaching procedure was performed by following a standard operating procedure outlined in Schobben et al., 2020. Each of the eight samples from the Chuskuna Formation were dosed with one mL of boiling concentrated HCl. They were allowed to react for one minute before being centrifuged and decanted into new 10 mL centrifuge tubes. The leached powder from the Chuskuna Formation was properly disposed of. In new 10 mL centrifuge tubes 100 µL of the leach solutions were added to 8.8 mL of 2% HNO_3. One mL of 100 ppb Sc was added to the centrifuge tubes as a spike for the analysis. The solutions were analyzed with the assistance of Tim Mock at the Carnegie Institution for Science on an iCap ICP-MS. Six standards with the same Sc spike and 0, 1, 10, 50, 200, 500 ppb Fe were used to calibrate the instrument for analysis.

Thallium Isotope Analysis Further analysis of the samples was completed by sending approximately one gram of the powdered sample from the Chuskuna Formation to the Woods Hole Oceanographic Institution for a thallium isotope analysis. This procedure was performed by Yunchao Shu under the guidance of Chadlin Ostrander. The shales were leached overnight in 2 M nitric acid. This is shown to liberate thallium from pyrite, which is the predominant thallium host in shales formed under anoxic conditions. It is this pyrite-bound thallium that is shown to closely track the seawater Tl isotope composition today. In oxidizing conditions thallium reacts with manganese, which removes the heavier-mass thallium isotope from seawater, driving the globally homogeneous seawater thallium isotope composition to a lighter value. This isotopic ratio is preserved in organic-rich marine sediments today, which are deposited under anoxic conditions (Ostrander et al., 2020).

Results

Whole rock data from the shale dissolution procedure is shown in a table containing the Chuskuna Formation and the formations of the White Sea region (Appendix 1). Standard deviations for each element are shown on the bottom row as calculated from standards. Those deviations represent the precision of the measurement for each element. Concentrations from this table were used to calculate the ratios plotted in the figure below (Fig. 8). This figure shows elemental ratios (found in Appendix 2), plotted versus the height of the samples within the formations. The dotted line is the composition for the upper continental crust (Rudnick and Gao, 2003). The metals are plotted against aluminum in order to understand the enrichments that occur in the water column over the presumed average continental flux to the oceans. The % carbonate and % sulfur from the acidification and CRS procedure are reported in a separate table below (Appendix 3).

Iron speciation data are shown below in two types of plots (Fig 9). The two upper plots show data from the Zimnie Gory and Era formations (Fig. 9a). The two lower plots show data from the Chuskuna Formation (Fig. 9b)(Appendix 4). Two different ratios are plotted for each locality. For each location, the plots on the left show the ratio between the highly reactive iron (Fe_{HR}) and the total iron (Fe_T). The Fe_{HR} ratio in the Chuskuna formation includes the measured poorly reactive silicate phase (Fe_{PRS}). The boundary between oxic and anoxic is a ratio of 0.38 (Bennett

and Canfield, 2020). The plots on the right of each formation show the ratio between the iron in pyrite (Fe_{py}) and the highly reactive iron. The boundary between ferruginous and euxinic is 0.80 (Bennett and Canfield, 2020). Highly reactive iron was determined by the sum of the iron in the carbonates, oxides, and magnetite, (as well as silicate for the Chuskuna Formation) as measured by the iron speciation analysis. The total iron was determined as part of the shale dissolution. The iron in pyrite was calculated stoichiometrically using the total iron and the % sulfur from the CRS analysis. The iron in the silicate phase was calculated for the Zimnie Gory and Erga formations, but for the Chuskuna Formation, the highly reactive fraction (extractable with boiling, concentrated HCl) was determined through an additional extraction step (Appendix 4).

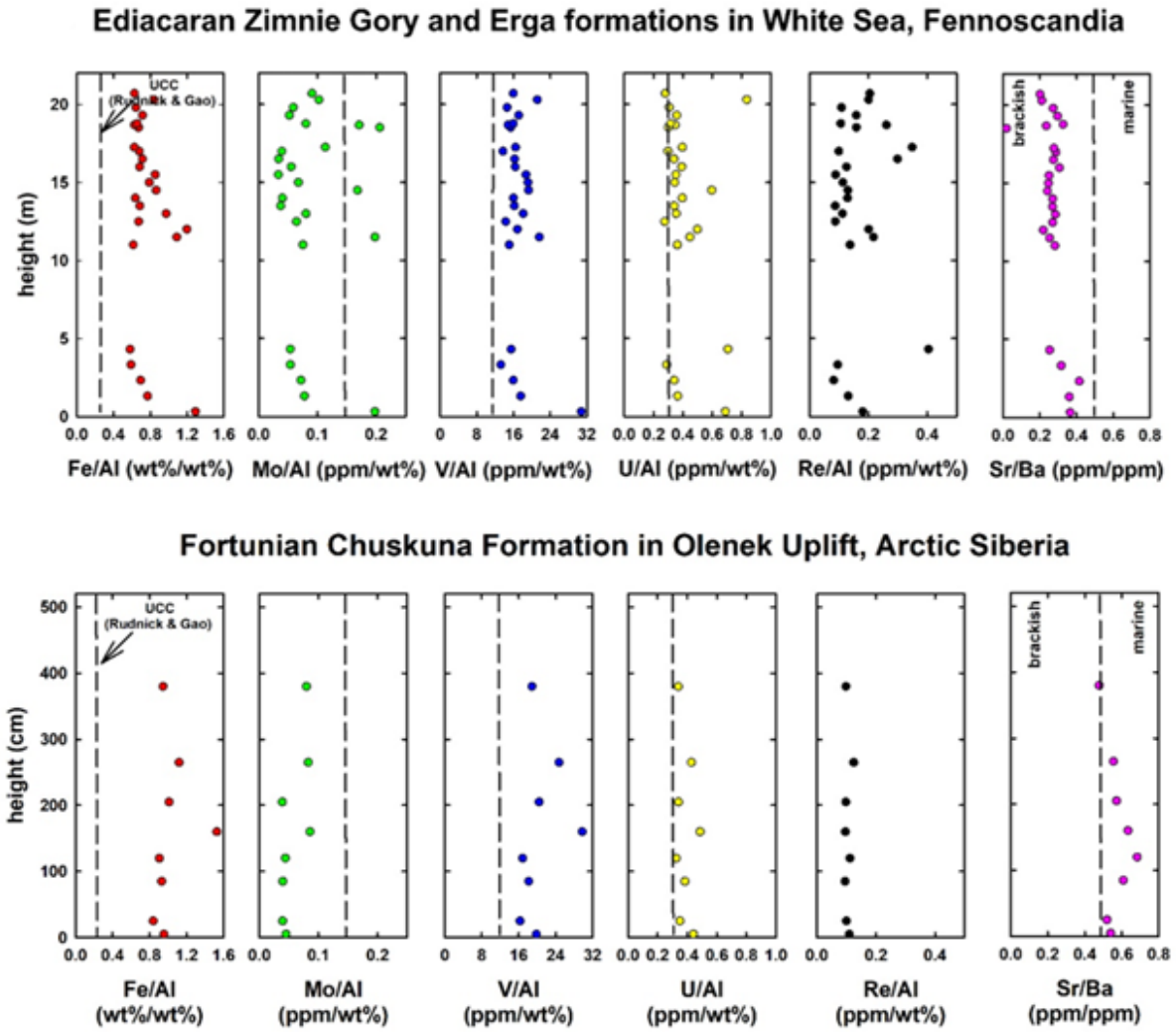

Figure 8: Elemental data from whole rock analysis plotted vs. Al. The dashed line represents the composition of the upper continental crust from Rudnick and Gao, 2003.

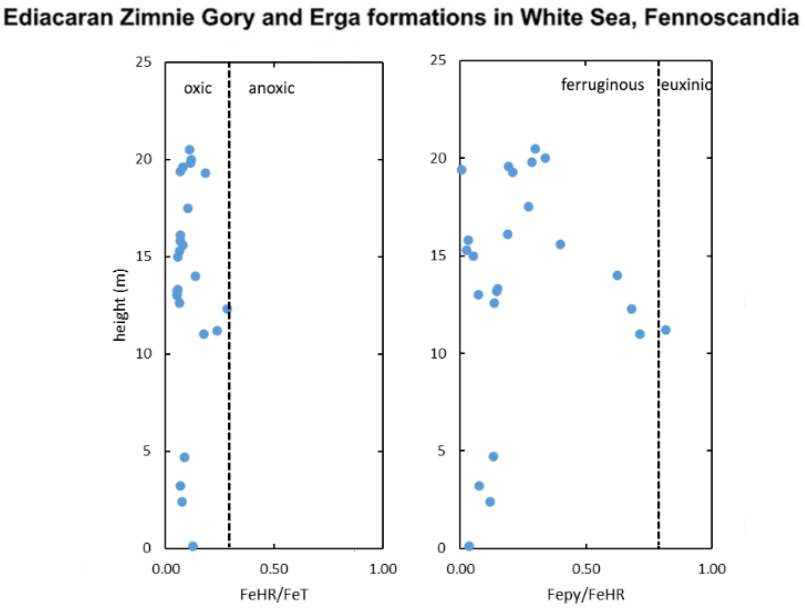

Figure 9a: Zimnie Gory and Erga formations Fe Speciation Data

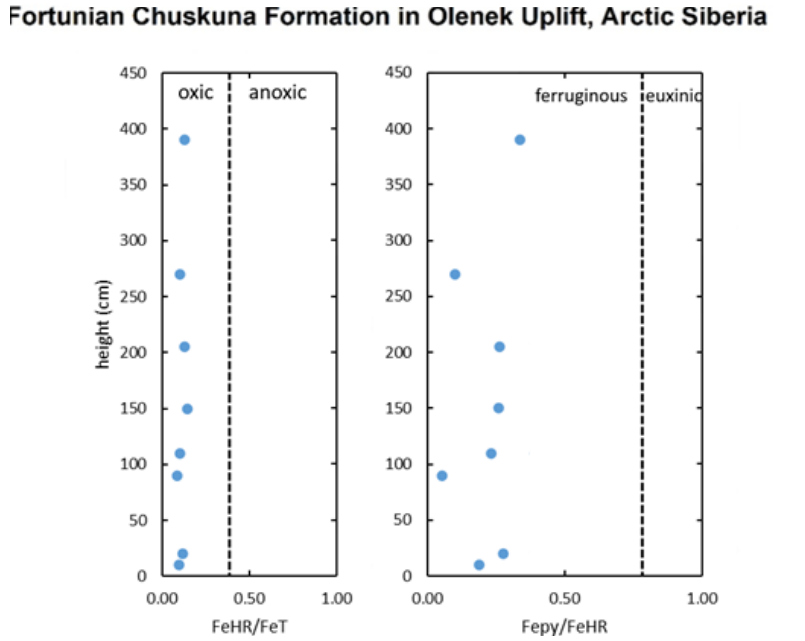

Figure 9b: Chuskuna Formation Fe Speciation Data

Discussion

The excellent preservation of the fossils in both the White Sea and Olenek Uplift could be explained by the sedimentology of the regions. For both of the regions, the lithofacies were deposited in prodelta environments. At a location such as this, a storm event has the potential to rapidly bury the organisms in the water column. This would create a barrier between the oxygen in the water column and the now buried organisms, serving as a possible explanation for the exceptional preservation of the fossils. Possible evidence for a storm event could be seen in thin section images of the Chuskuna Formation (Fig. 10), as there are broken fossil fragments, indicating rapid sediment transport.

The strontium/barium ratios of the rocks of the Chuskuna Formation indicate marine conditions (Fig 8). This is consistent with the geology of the locality, as the depositional environment is interpreted as prodelta. The strontium/barium ratios of the rocks of the Zimnie Gory and Erga formations indicate brackish conditions. A modern analog for this would be the Chesapeake Bay, where fresh water interacts with saltwater.

Most metals are soluble in their reduced form, so they would remain in the water column in anoxic or euxinic conditions. The presence of any oxygen would allow for the metals to react, to form oxides, and be sequestered into sediment. In anoxic conditions the metals would have no oxygen to react with, but they can get concentrated with sulfide minerals and hence be trapped in the sediments. The lack of metal enrichments relative to the upper continental crust would be consistent with oxic conditions in the depositional environment, such that the metal inventory would not grow in the ocean (Fig. 8). However, this seems inconsistent with the exceptional fossil preservations, the thallium isotope data, and the abundance of glauconite in thin sections. Oxic environments support life that is able to decompose organisms, so recently deceased organisms are less likely to remain in the sediment long enough to be fossilized.

One possibility for the lack of metal enrichment is long term euxinia in the late Ediacaran and early Fortunian. Uranium isotope and metal studies of this time interval indicate that euxinic conditions persisted for tens of millions of years, resulting in the depletion of the metal inventory (Cherry et al., 2022). Metals behave in a similar manner in anoxic and euxinic conditions, as the presence of oxygen is very low in both cases. Long term euxinia could cause the metal inventory of the oceans to be depleted. This means that at the time of formation for the Zimnie Gory, Erga, and Chuskuna formations, if there were anoxic conditions, the prolonged euxinia prior would leave low concentration of metal in the ocean to get trapped in the sediments.

The predominant host for thallium in shales formed under anoxic condition is pyrite. Pyrite bound thallium has been shown to closely track the thallium isotope composition today (Ostrander et al., 2020). The shale from the Chuskuna Formation has values that overlap with the upper continental crust (about -2 +/- 0.3 epsilon units) (Appendix 5). This data alone indicates a limited seafloor manganese burial, resulting in anoxic conditions. This is further supported by the low manganese abundance that was measured by the shale dissolution. This would indicate that there was a broadly anoxic (or euxinic) global ocean with a largely unfractionated seawater thallium isotope composition. However, with only a limited section to work from it can be difficult to determine if thallium represents a globally homogenous open ocean. It is possible that the thallium isotope data reflect an isolated basin, with its own near-crustal seawater isotope composition.

Figure 10: Thin section from the Chuskuna Formation (plane polarized light). Glauconite is the green mineral, seen primarily on the left side of the image.

When looking at the iron speciation data, strong oxic signals are seen in the Fe_{HR}/Fe_T ratios. The ~15-20% carbonate in the samples (which is a high percentage for shale) was not reflected in the iron speciation data, as the iron in the carbonate phase was low. While contradicting at first, this could be explained by the abundance of glauconite that can be seen in thin section images. The iron silicate fraction (Fe_{PRS}) is usually calculated as the subtraction of the rest of the iron phases from the total, however it was measured for the Chuskuna Formations due to the visible large amount of glauconite in the sample. (Fig. 10). The measured Fe_{PRS} was ~0.5-0.6 wt.%, while that is is a large amount of glauconite, it is not enough to account for the total iron in the sample (~6-7 wt.%) (Appendix 4). It seems that the majority of the iron is in detrital and non-authigenic phases, meaning that an anoxic signal is potentially being masked by very high sedimentation rates. Looking closer at the exceptionally high zircon and titanium concentrations (minerals concentrated in coarser-grained detrital sediment), support that there could have been high sedimentation rates (Appendix 1). This interpretation explains the elevated Fe/Al, allows for the thallium isotope to be interpreted as signals of anoxia, and leaves the potential for the low metal abundances to be caused by extended euxinia.

Conclusions

The hypothesis of anoxia in the sediments is not supported by the lack of discernible metal enrichment that would be expected with anoxic/euxinic conditions. However, this is inconsistent with the expectation that the sediments would likely need to be anoxic to preserve the fossil remains and impressions but may be the result of ferruginous rather than sulfidic conditions and the long-term depletion of metals from the oceanic inventory. The strontium/barium ratios of the rocks in the formations indicate marine and brackish conditions, which is consistent with the geological interpretation. Thallium isotope measurements point towards a broadly global anoxic ocean. Iron speciation reveals low iron abundance in the measured phases, however high iron abundance measured from the shale dissolution procedure indicates that there could have been high sedimentation rates.

Acknowledgements

I would like to thank Alan J. Kaufman, Geoffrey Gilleaudeau, Dmitriy Grazhdankin, Chadlin Ostrander, Olga Dantes, and Tim Mock for all their help and contributions to this project.

Bibliography

Algeo, T. J., & Liu, J. (2020). A re-assessment of elemental proxies for paleoredox analysis. *Chemical Geology*, *540*, 119549. https://doi.org/10.1016/j.chemgeo.2020.119549

Bennett, W. W., & Canfield, D. E. (2020). Redox-sensitive trace metals as paleoredox proxies: A review and analysis of data from modern sediments. *Earth-Science Reviews*, *204*, 103175. https://doi.org/10.1016/j.earscirev.2020.103175

Bobrovskiy, I., Hope, J. M., Ivantsov, A., Nettersheim, B. J., Hallmann, C., & Brocks, J. J. (2018). Ancient steroids establish the Ediacaran fossil Dickinsonia as one of the earliest animals. Science, 361(6408), 1246–1249. https://doi.org/10.1126/science.aat7228

Butterfield, N. J. (2003). Exceptional fossil preservation and the Cambrian explosion. *Integrative and Comparative Biology*, *43*(1), 166–177. https://doi.org/10.1093/icb/43.1.166

Canfield, D. E., Raiswell, R., Westrich, J. T., Reaves, C. M., & Berner, R. A. (1986). The use of chromium reduction in the analysis of reduced inorganic sulfur in sediments and shales. *Chemical Geology*, *54*(1–2), 149–155. https://doi.org/10.1016/0009-2541(86)90078-1

Cherry, L. B., Gilleaudeau, G. J., Grazhdankin, D. V., Romaniello, S. J., Martin, A. J., & Kaufman, A. J. (2022). A diverse Ediacara assemblage survived under low-oxygen conditions. *Nature Communications*, *13*(1), 7306. https://doi.org/10.1038/s41467-022-35012-y

Droser, M. L., Tarhan, L. G., & Gehling, J. G. (2017). The rise of animals in a changing environment: Global ecological innovation in the late Ediacaran. *Annual Review of Earth and Planetary Sciences*, *45*(1), 593–617. https://doi.org/10.1146/annurev-earth-063016-015645

Grazhdankin, D. (2004). Patterns of distribution in the Ediacaran biotas: Facies versus biogeography and evolution. *Paleobiology*, *30*(2), 203–221. https://doi.org/10.1666/0094-8373(2004)030<0203:PODITE>2.0.CO;2

Grazhdankin, D. V. (2003). Structure and depositional environment of the Vasyugan Horizon (Upper bathonian–oxfordian) in the Aleksandrovskoe arch area (West siberia). *Stratigraphy And Geological Correlation*, *11*(4), 313–331.

Grazhdankin, D. V., Marusin, V. V., Izokh, O. P., Karlova, G. A., Kochnev, B. B., Markov, G. E., Nagovitsin, K. E., Sarsembaev, Z., Peek, S., Cui, H., & Kaufman, A. J. (2020). Quo vadis, Tommotian? *Geological Magazine*, *157*(1), 22–34. https://doi.org/10.1017/S0016756819001286

Hou, X., Ramskold, L., & Bergstrom, J. (1991). Composition and preservation of the Chengjiang fauna -a Lower Cambrian soft-bodied biota. *Zoologica Scripta*, *20*(4), 395–411. https://doi.org/10.1111/j.1463-6409.1991.tb00303.x

Martin, M. W., Grazhdankin, D. V., Bowring, S. A., Evans, D. A. D., Fedonkin, M. A., & Kirschvink, J. L. (2000). Age of neoproterozoic bilatarian body and trace fossils, white sea, russia: Implications for metazoan evolution. *Science*, *288*(5467), 841–845. https://doi.org/10.1126/science.288.5467.841

Ostrander, C. M., Owens, J. D., Nielsen, S. G., Lyons, T. W., Shu, Y., Chen, X., Sperling, E. A., Jiang, G., Johnston, D. T., Sahoo, S. K., & Anbar, A. D. (2020). Thallium isotope ratios in shales from South China and northwestern Canada suggest widespread O2 accumulation in marine bottom waters was an uncommon occurrence during the Ediacaran Period. Chemical Geology, 557, 119856. https://doi.org/10.1016/j.chemgeo.2020.119856

Rudnick, R. L., & Gao, S. (2003). Composition of the continental crust. In Treatise on Geochemistry (pp. 1–64). Elsevier. https://doi.org/10.1016/B0-08-043751-6/03016-4

Schobben, M., Foster, W. J., Sleveland, A. R. N., Zuchuat, V., Svensen, H. H., Planke, S., Bond, D. P. G., Marcelis, F., Newton, R. J., Wignall, P. B., & Poulton, S. W. (2020). A nutrient control on marine anoxia during the end-Permian mass extinction. Nature Geoscience, 13(9), 640–646. https://doi.org/10.1038/s41561-020-0622-1

Walcott, C. (1912). Middle Cambrian Branchiopoda, Malacostraca, Trilobita and Merostomata. *Smithsonian Miscellaneous Collections*, *57*(6), 148–228. https://doi.org/10.1086/621642

Appendix

Sample #	^{23}Na (KED)	^{25}Mg (KED)	^{27}Al (KED)	^{31}P (KED)	^{39}K (KED)	^{44}Ca (KED)	^{47}Ti (KED)	^{51}V (KED)	^{52}Cr (KED)
Chuskuna	All concentrations in rock ppm								
1221-01	3228.15	18906.63	70464.73	367.00	40640.17	12892.57	8387.76	139.78	123.65
1221-02	3751.65	19023.02	72137.21	449.23	38482.16	11860.01	8030.51	117.44	108.39
1221-05	2431.22	18745.38	70235.12	310.18	40372.95	12254.06	6957.86	127.56	106.78
1221-07	2891.21	17845.69	66062.33	363.20	36473.67	12806.11	6868.58	111.40	96.88
1221-10	2502.59	11003.54	42056.35	350.28	30660.08	13738.07	7001.04	124.99	107.54
1221-13	3361.16	17379.18	63929.62	434.11	38040.26	14005.38	8153.34	130.43	113.35
1221-16	3999.62	14303.09	56080.32	453.15	36218.26	10158.44	9027.74	138.43	118.79
1221-20	4117.60	15989.23	61470.45	484.40	34492.55	10834.85	8151.80	115.89	100.17
White Sea									
1 0123.2	5254.06	7767.17	40510.86	2309.75	24633.35	10537.70	5537.14	124.64	86.96
2 0123.2	7517.59	13715.80	64979.69	565.58	28019.44	8004.60	4966.46	114.01	77.82
3 0123.2	6872.25	16652.96	76871.75	549.90	31483.07	8410.28	4991.50	122.64	86.46
4 0123.2	9434.74	18817.62	89634.14	668.25	34077.65	7814.22	5381.51	118.83	85.72
5 0123.2	8417.21	16493.53	88035.82	552.69	35977.86	7599.21	5384.20	136.11	83.72
6 0123.2	8174.38	13123.42	72011.67	293.13	28676.71	6027.51	4373.67	108.44	67.81
7 0123.2	8833.16	9150.61	55387.14	269.13	27380.96	5558.94	5028.29	119.73	77.03
8 0123.2	9626.76	9731.99	58990.84	269.32	26770.15	5816.40	4800.57	99.30	68.90
9 0123.2	8842.54	15537.88	80326.30	300.01	33251.13	6668.74	5360.60	114.94	79.69
10 0123.2	8058.59	11722.22	64651.65	270.30	31790.04	6074.59	5511.26	117.09	80.18
11 0123.2	8213.91	10516.42	60399.23	235.89	27320.48	5577.76	4651.43	97.62	65.43
12 0123.2	8342.76	11237.37	62827.81	231.69	26962.95	5668.87	4582.70	100.48	67.34
13 0123.2	7961.45	7234.79	42020.91	236.10	21231.45	6378.26	3882.73	81.01	56.59
14 0123.2	8463.73	8828.16	49002.10	243.94	26189.53	4821.86	4630.65	93.79	70.42
15 0123.2	7892.35	10851.54	55558.90	250.41	26526.38	6138.79	4792.37	104.02	70.07
16 0123.2	8878.87	14618.16	66763.02	527.48	27953.86	7097.59	4916.98	109.36	74.01
17 0123.2	6666.58	14293.79	73679.27	252.43	31362.35	5808.35	4792.19	119.56	75.88
18 0123.2	5434.13	15736.90	79853.71	221.89	33790.48	7395.82	4373.67	109.28	69.10
19 0123.2	8858.07	12384.90	67779.10	471.24	28618.23	8871.26	5101.42	111.38	71.08
20 0123.2	7485.45	10337.36	58397.52	358.51	25622.18	8896.68	4017.18	89.73	59.38
21 0123.2	9457.30	11748.77	70736.22	674.57	29440.24	14668.75	4906.95	104.67	71.63
22 0123.2	6105.95	17968.89	81502.30	572.47	33270.12	9511.92	5421.94	129.97	92.61
23 0123.2	7916.25	14077.03	72113.60	518.16	30663.93	8438.18	5444.75	123.35	87.84
24 0123.2	5834.75	16952.61	88607.03	1017.93	35253.34	7541.12	4916.81	129.18	87.20
25 0123.2	4241.94	9097.17	50641.30	226.44	25056.98	6426.72	3881.70	107.20	67.82
26 0123.2	4568.87	14978.52	79568.68	261.40	33037.28	6765.21	4395.61	127.04	79.92
RSD (%)	2.10%	1.00%	1.40%	2.20%	0.80%	1.90%	1.20%	1.30%	1.60%

Appendix 1: Chuskuna Formation and White Sea region whole rock major, minor, trace, and REE abundance (in ppm). RSD for each element reported in the bottom row.

Sample #	^{55}Mn (KED)	^{56}Fe (KED)	^{59}Co (KED)	^{60}Ni (KED)	^{65}Cu (KED)	^{68}Zn (KED)	^{75}As (KED)	^{77}Se (KED)	^{85}Rb (KED)
Chuskuna	All concentrations in rock ppm								
1221-01	306.24	67259.58	27.42	49.87	12.40	171.93	4.05	5.47	149.79
1221-02	289.36	60545.66	22.26	42.36	12.68	140.27	4.65	7.80	146.70
1221-05	282.59	65369.02	29.11	48.94	19.06	153.14	4.79	10.65	145.03
1221-07	290.81	59791.44	22.57	42.54	17.52	147.70	3.61	10.84	140.36
1221-10	331.62	64218.94	24.48	57.99	19.33	148.26	3.01	4.87	64.31
1221-13	350.92	64619.09	23.46	46.21	49.17	153.78	5.98	9.01	104.23
1221-16	319.53	62760.07	23.12	47.65	19.32	116.40	3.57	7.96	91.82
1221-20	308.86	58048.92	24.98	41.34	18.50	112.66	4.65	11.51	105.10
White Sea									
1 0123.2	587.48	52327.11	18.09	38.55	8.37	140.89	6.21	7.08	41.27
2 0123.2	452.43	49978.24	19.58	34.45	7.72	135.53	6.58	7.44	97.21
3 0123.2	468.76	53431.24	17.25	36.18	5.90	138.22	4.15	7.92	124.42
4 0123.2	476.34	52797.78	18.43	34.56	27.48	143.42	6.16	10.72	147.71
5 0123.2	290.31	50903.46	13.56	31.55	10.11	136.05	7.51	11.59	169.12
6 0123.2	245.02	44245.83	11.11	27.59	15.75	119.96	8.64	8.40	132.96
7 0123.2	269.52	60209.83	20.47	37.66	16.38	137.81	21.25	3.53	70.56
8 0123.2	241.03	70693.29	17.08	36.32	40.75	131.22	17.83	4.70	71.98
9 0123.2	307.14	54032.08	16.95	31.84	24.45	153.02	6.12	9.22	133.19
10 0123.2	316.46	62879.04	23.20	34.33	19.93	145.04	3.18	5.39	108.68
11 0123.2	234.94	41375.42	10.90	24.50	22.95	120.22	2.48	5.61	99.31
12 0123.2	252.95	40041.52	11.76	24.23	5.26	116.23	3.58	4.92	98.47
13 0123.2	196.36	36335.35	10.30	24.34	11.16	119.53	4.92	4.62	65.42
14 0123.2	221.78	38631.23	10.16	24.05	49.54	123.16	2.04	4.43	75.10
15 0123.2	257.46	47377.36	15.51	28.69	11.95	127.88	2.65	4.50	80.52
16 0123.2	472.59	45685.16	15.51	29.25	32.92	132.45	5.25	6.46	89.97
17 0123.2	277.29	52532.00	15.49	31.82	6.81	127.06	3.32	7.47	136.30
18 0123.2	257.82	54192.66	26.35	39.87	20.19	147.77	13.82	6.34	155.86
19 0123.2	511.63	42406.04	14.56	27.88	7.54	128.31	10.44	7.33	99.21
20 0123.2	371.56	39297.13	21.36	27.92	33.69	912.86	12.18	5.76	88.66
21 0123.2	295.07	44383.85	17.37	29.57	20.02	129.19	11.02	8.52	112.79
22 0123.2	470.58	53509.54	14.93	34.13	26.49	140.93	3.08	9.33	127.55
23 0123.2	451.35	51481.33	16.90	35.27	33.61	141.19	6.93	7.20	112.06
24 0123.2	360.91	57022.24	20.12	36.66	44.06	135.45	11.68	16.10	173.38
25 0123.2	241.54	42599.28	12.56	26.75	15.90	124.61	6.36	4.35	81.96
26 0123.2	310.86	49901.08	12.81	29.62	13.66	221.58	6.18	8.52	160.29
RSD (%)	0.40%	0.60%	0.40%	1.20%	0.80%	1.10%	1.40%	4.50%	0.70%

Appendix 1 (continued): Chuskuna Formation and White Sea region whole rock major, minor, trace, and REE abundance (in ppm). RSD for each element reported in the bottom row.

Sample #	^{88}Sr (KED)	^{89}Y (KED)	^{91}Zr (KED)	^{98}Mo (KED)	^{111}Cd (KED)	^{121}Sb (KED)	^{133}Cs (KED)	^{137}Ba (KED)	^{139}La (KED)
Chuskuna	All concentrations in rock ppm								
1221-01	116.20	16.66	289.68	0.32	0.04	0.21	10.10	215.17	36.86
1221-02	115.73	20.46	277.35	0.28	0.03	0.18	10.20	222.37	41.45
1221-05	128.52	30.30	502.06	0.28	0.04	0.25	11.33	211.16	41.40
1221-07	132.19	26.46	389.94	0.29	0.03	0.19	9.90	193.37	39.69
1221-10	103.57	11.15	338.50	0.36	0.03	0.17	6.20	163.45	14.53
1221-13	117.89	23.38	378.39	0.25	0.04	0.18	8.70	205.93	29.70
1221-16	98.27	17.62	404.25	0.46	0.05	0.28	7.65	177.04	24.65
1221-20	97.71	23.51	350.78	0.49	0.04	0.22	8.53	204.46	29.80
White Sea									
1 0123.2	61.52	10.77	186.83	0.80	0.04	0.25	1.54	167.91	12.16
2 0123.2	78.55	14.20	148.28	0.50	0.03	0.34	4.35	217.81	29.11
3 0123.2	95.66	17.00	154.96	0.55	0.02	0.24	4.85	230.36	36.39
4 0123.2	99.25	24.36	182.04	0.48	0.02	0.29	5.35	313.12	44.46
5 0123.2	90.08	23.55	189.90	0.47	0.03	0.33	7.56	354.55	44.41
6 0123.2	86.69	18.10	161.77	0.54	0.04	0.34	5.38	306.64	39.89
7 0123.2	62.98	8.21	190.38	1.10	0.06	0.42	4.05	248.60	19.72
8 0123.2	67.17	10.68	202.81	3.78	0.04	0.70	4.11	306.39	17.54
9 0123.2	93.80	20.38	199.92	0.52	0.02	0.29	6.73	346.22	38.32
10 0123.2	76.57	13.91	203.07	0.52	0.03	0.26	6.03	268.53	26.79
11 0123.2	70.06	11.64	154.96	0.23	0.02	0.22	4.96	259.71	28.35
12 0123.2	78.04	12.09	159.37	0.25	0.02	0.23	5.02	288.26	25.84
13 0123.2	44.72	9.32	157.98	0.71	0.02	0.35	3.10	185.03	18.74
14 0123.2	55.24	8.89	169.56	0.33	0.02	0.21	4.27	223.60	18.60
15 0123.2	65.16	9.87	179.72	0.19	0.02	0.25	4.69	258.95	19.53
16 0123.2	82.29	15.23	188.74	0.37	0.02	0.28	3.90	267.70	25.48
17 0123.2	78.02	16.79	173.18	0.25	0.02	0.24	6.59	283.72	33.99
18 0123.2	78.50	19.35	167.63	0.32	0.03	0.38	7.19	272.43	33.43
19 0123.2	79.82	16.17	178.59	0.77	0.02	0.29	3.93	287.54	30.61
20 0123.2	276.98	13.68	164.06	1.20	0.03	0.69	3.52	14215.14	26.10
21 0123.2	79.18	20.58	226.82	1.21	0.06	0.69	4.28	335.23	32.45
22 0123.2	86.60	18.55	176.08	0.65	0.02	0.23	5.50	264.56	38.77
23 0123.2	79.85	14.79	169.87	0.38	0.05	0.30	4.82	267.93	32.64
24 0123.2	88.34	29.76	152.01	0.52	0.02	0.42	6.94	323.68	54.41
25 0123.2	43.64	8.74	132.51	0.52	0.03	0.36	4.26	206.28	21.05
26 0123.2	66.91	19.19	156.02	0.72	0.16	0.38	7.26	331.87	42.95
RSD (%)	0.60%	56.70%	0.60%	2.90%	1.50%	1.50%	0.50%	0.60%	1.00%

Appendix 1 (continued): Chuskuna Formation and White Sea region whole rock major, minor, trace, and REE abundance (in ppm). RSD for each element reported in the bottom row.

Sample #	^{140}Ce (KED)	^{141}Pr (KED)	^{144}Nd (KED)	^{147}Sm (KED)	^{153}Eu (KED)	^{157}Gd (KED)	^{159}Tb (KED)	^{163}Dy (KED)	^{165}Ho (KED)
Chuskuna	All concentrations in rock ppm								
1221-01	61.71	6.42	22.61	4.22	0.85	3.61	0.58	3.93	0.84
1221-02	78.34	8.73	32.72	6.30	1.19	5.24	0.79	4.98	1.02
1221-05	87.03	9.85	38.51	8.11	1.41	7.41	1.22	7.71	1.51
1221-07	82.54	9.51	37.33	7.68	1.41	6.74	1.06	6.52	1.26
1221-10	32.48	3.83	15.49	3.33	0.67	3.00	0.52	3.41	0.68
1221-13	64.55	7.70	30.97	6.56	1.34	5.90	1.00	6.47	1.29
1221-16	48.26	5.41	20.69	4.22	0.88	3.94	0.68	4.61	0.94
1221-20	64.90	7.45	29.77	6.41	1.33	5.87	0.96	6.22	1.24
White Sea									
1 0123.2	28.22	3.94	17.97	4.76	1.11	4.58	0.65	3.50	0.60
2 0123.2	56.01	6.60	25.58	4.97	1.00	4.11	0.59	3.53	0.68
3 0123.2	71.73	7.93	29.92	5.51	1.08	4.48	0.66	4.03	0.80
4 0123.2	91.71	10.20	39.48	7.64	1.54	6.52	0.95	5.80	1.14
5 0123.2	90.62	10.15	39.46	7.83	1.50	6.46	0.95	5.78	1.13
6 0123.2	81.39	8.94	34.07	6.31	1.19	4.99	0.73	4.40	0.87
7 0123.2	37.28	4.38	16.30	2.91	0.55	2.27	0.34	2.11	0.42
8 0123.2	36.81	4.21	16.31	3.30	0.64	2.72	0.44	2.93	0.61
9 0123.2	81.49	9.20	35.01	6.63	1.27	5.30	0.81	5.13	1.05
10 0123.2	53.58	5.85	21.92	3.94	0.75	3.13	0.49	3.33	0.70
11 0123.2	54.04	6.08	22.58	3.91	0.72	2.97	0.44	2.79	0.56
12 0123.2	50.61	5.60	20.75	3.76	0.70	2.93	0.46	3.01	0.62
13 0123.2	39.07	4.43	16.99	3.12	0.60	2.50	0.37	2.30	0.45
14 0123.2	36.44	4.44	17.01	3.13	0.59	2.43	0.37	2.32	0.47
15 0123.2	39.21	4.51	17.12	3.11	0.60	2.48	0.39	2.59	0.54
16 0123.2	52.15	5.99	23.50	4.78	0.98	4.13	0.63	3.97	0.80
17 0123.2	69.96	7.87	29.79	5.38	1.02	4.24	0.65	4.14	0.85
18 0123.2	66.10	7.08	26.07	4.57	0.87	3.85	0.65	4.55	0.97
19 0123.2	61.66	6.71	25.83	4.99	0.97	4.18	0.63	3.96	0.80
20 0123.2	52.16	5.85	22.44	4.32	1.05	3.69	0.53	3.32	0.66
21 0123.2	66.83	7.68	30.96	6.43	1.25	5.57	0.82	4.96	0.96
22 0123.2	77.66	8.80	33.48	6.34	1.26	5.18	0.77	4.69	0.94
23 0123.2	64.29	7.16	27.05	5.04	0.97	4.06	0.60	3.64	0.72
24 0123.2	117.35	13.72	56.29	12.12	2.41	10.16	1.39	7.76	1.40
25 0123.2	42.62	4.81	18.14	3.28	0.60	2.47	0.36	2.27	0.45
26 0123.2	87.13	9.46	35.31	6.24	1.16	4.77	0.72	4.54	0.93
RSD (%)	0.90%	1.10%	1.10%	1.00%	1.70%	1.00%	1.30%	0.70%	1.80%

Appendix 1 (continued): Chuskuna Formation and White Sea region whole rock major, minor, trace, and REE abundance (in ppm). RSD for each element reported in the bottom row.

Sample #	^{166}Er (KED)	^{169}Tm (KED)	^{172}Yb (KED)	^{175}Lu (KED)	^{178}Hf (KED)	^{182}W (KED)	^{187}Re (KED)	^{205}Tl (KED)	^{208}Pb (KED)	^{232}Th (KED)	^{238}U (KED)
Chuskuna	All concentrations in rock ppm										
1221-01	2.66	0.42	2.88	0.41	7.20	1.99	0.001	0.43	8.88	10.24	3.11
1221-02	3.17	0.48	3.33	0.47	6.83	1.89	0.001	0.41	7.18	11.27	2.53
1221-05	4.39	0.63	4.21	0.58	11.68	1.50	0.001	0.41	11.57	13.25	2.71
1221-07	3.65	0.52	3.45	0.47	9.57	1.43	0.001	0.38	8.68	12.63	2.15
1221-10	2.00	0.29	1.97	0.27	8.88	1.47	0.000	0.36	7.85	4.64	2.05
1221-13	3.79	0.55	3.68	0.51	9.14	1.52	0.001	0.39	8.42	8.59	2.18
1221-16	2.82	0.42	2.81	0.39	10.48	1.74	0.001	0.40	10.05	7.46	2.40
1221-20	3.57	0.52	3.42	0.47	8.59	1.46	0.001	0.36	11.67	8.56	2.09
White Sea											
1 0123.2	1.52	0.20	1.27	0.18	7.42	1.94	0.001	0.56	7.09	4.81	2.80
2 0123.2	2.01	0.29	2.00	0.28	4.21	1.44	0.001	0.54	7.34	10.29	2.37
3 0123.2	2.42	0.36	2.44	0.35	4.50	1.45	0.001	0.60	6.80	13.06	2.62
4 0123.2	3.37	0.49	3.32	0.47	4.80	1.41	0.001	0.62	7.31	16.61	2.60
5 0123.2	3.34	0.49	3.36	0.47	4.95	1.59	0.004	0.72	8.49	18.54	6.22
6 0123.2	2.63	0.40	2.74	0.39	4.27	1.27	0.001	0.59	18.52	15.08	2.62
7 0123.2	1.32	0.20	1.42	0.20	5.65	1.62	0.001	0.68	32.93	7.14	2.49
8 0123.2	1.90	0.30	2.13	0.31	5.45	1.40	0.001	0.95	23.41	7.67	2.94
9 0123.2	3.23	0.48	3.35	0.48	5.21	1.57	0.001	0.65	8.07	14.70	2.23
10 0123.2	2.23	0.34	2.36	0.33	5.26	1.68	0.001	0.65	6.80	10.58	2.29
11 0123.2	1.76	0.27	1.86	0.27	4.23	1.40	0.001	0.55	6.38	10.28	2.06
12 0123.2	1.96	0.30	2.13	0.30	4.30	1.35	0.001	0.53	6.70	10.07	2.49
13 0123.2	1.36	0.21	1.42	0.20	6.27	1.69	0.001	0.51	10.70	7.38	2.51
14 0123.2	1.45	0.22	1.53	0.22	4.57	1.35	0.001	0.52	5.40	8.01	1.69
15 0123.2	1.71	0.27	1.91	0.28	4.63	1.33	0.000	0.56	5.67	7.74	1.96
16 0123.2	2.40	0.36	2.47	0.35	4.82	1.15	0.001	0.55	8.17	9.61	2.62
17 0123.2	2.61	0.39	2.75	0.39	4.51	1.38	0.002	0.60	6.77	14.13	2.50
18 0123.2	3.06	0.46	3.26	0.46	4.20	1.21	0.001	0.73	14.43	15.82	2.39
19 0123.2	2.38	0.36	2.47	0.35	5.16	1.37	0.002	0.58	9.68	11.66	2.69
20 0123.2	1.98	0.29	2.04	0.29	4.16	1.04	0.001	0.56	23.53	10.27	1.77
21 0123.2	2.85	0.42	2.91	0.41	5.94	1.31	0.002	0.62	20.54	12.84	2.46
22 0123.2	2.79	0.42	2.89	0.41	4.56	1.36	0.001	0.62	5.73	13.99	2.58
23 0123.2	2.17	0.32	2.24	0.33	4.50	1.40	0.001	0.64	10.95	11.92	2.58
24 0123.2	3.87	0.54	3.54	0.50	4.00	1.36	0.001	0.69	11.29	18.70	2.72
25 0123.2	1.39	0.21	1.47	0.21	3.97	1.16	0.001	0.55	12.91	8.17	4.23
26 0123.2	2.86	0.43	2.99	0.42	4.09	1.25	0.002	0.72	36.19	17.15	2.24
RSD (%)	1.10%	1.20%	1.20%	1.10%	1.20%	4.80%	0.90%	1.10%	5.40%	4.40%	1.30%

Appendix 1 (continued): Chuskuna Formation and White Sea region whole rock major, minor, trace, and REE abundance (in ppm). RSD for each element reported in the bottom row.

Sample #	Fe/Al	Mo/Al	V/Al	U/Al	Re/Al	Sr/Ba
Chuskuna						
1221-01	0.95	0.04	19.84	0.44	0.11	0.54
1221-02	0.84	0.04	16.28	0.35	0.10	0.52
1221-05	0.93	0.04	18.16	0.39	0.10	0.61
1221-07	0.91	0.04	16.86	0.32	0.11	0.68
1221-10	1.53	0.09	29.72	0.49	0.10	0.63
1221-13	1.01	0.04	20.40	0.34	0.10	0.57
1221-16	1.12	0.08	24.68	0.43	0.12	0.56
1221-20	0.94	0.08	18.85	0.34	0.10	0.48
White Sea						
1 0123.2	1.29	0.20	30.77	0.69	0.18	0.37
2 0123.2	0.77	0.08	17.55	0.36	0.13	0.36
3 0123.2	0.70	0.07	15.95	0.34	0.08	0.42
4 0123.2	0.59	0.05	13.26	0.29	0.10	0.32
5 0123.2	0.58	0.05	15.46	0.71	0.40	0.25
6 0123.2	0.61	0.08	15.06	0.36	0.14	0.28
7 0123.2	1.09	0.20	21.62	0.45	0.22	0.25
8 0123.2	1.20	0.64	16.83	0.50	0.20	0.22
9 0123.2	0.67	0.06	14.31	0.28	0.09	0.27
10 0123.2	0.97	0.08	18.11	0.35	0.11	0.29
11 0123.2	0.69	0.04	16.16	0.34	0.09	0.27
12 0123.2	0.64	0.04	15.99	0.40	0.13	0.27
13 0123.2	0.86	0.17	19.28	0.60	0.13	0.24
14 0123.2	0.79	0.07	19.14	0.35	0.11	0.25
15 0123.2	0.85	0.03	18.72	0.35	0.09	0.25
16 0123.2	0.68	0.06	16.38	0.39	0.13	0.31
17 0123.2	0.71	0.03	16.23	0.34	0.30	0.27
18 0123.2	0.68	0.04	13.68	0.30	0.10	0.29
19 0123.2	0.63	0.11	16.43	0.40	0.35	0.28
20 0123.2	0.67	0.21	15.36	0.30	0.16	0.02
21 0123.2	0.63	0.17	14.80	0.35	0.26	0.24
22 0123.2	0.66	0.08	15.95	0.32	0.11	0.33
23 0123.2	0.71	0.05	17.11	0.36	0.16	0.30
24 0123.2	0.64	0.06	14.58	0.31	0.11	0.27
25 0123.2	0.84	0.10	21.17	0.84	0.20	0.21
26 0123.2	0.63	0.91	15.97	0.28	0.20	0.20

Appendix 2: Elemental ratios plotted in figure 8. Data from appendix 1 used to calculate ratios. Fe and Al used values in wt.% to reduce number of zeros in final ratios.

Sample #	%carbonate	%sulfur
Chuskuna		
1221-01	14.69%	0.12%
1221-02	14.05%	0.17%
1221-05	16.15%	0.06%
1221-07	14.76%	0.14%
1221-10	16.88%	0.20%
1221-13	16.37%	0.19%
1221-16	14.51%	0.09%
1221-20	13.67%	0.24%
White Sea		
1 0123.2	19.37%	0.02%
2 0123.2	18.83%	0.05%
3 0123.2	21.31%	0.04%
4 0123.2	18.97%	0.02%
5 0123.2	17.95%	0.04%
6 0123.2	14.76%	0.36%
7 0123.2	15.75%	0.85%
8 0123.2	12.78%	0.98%
9 0123.2	15.42%	0.03%
10 0123.2	15.76%	0.02%
11 0123.2	15.68%	0.03%
12 0123.2	14.24%	0.03%
13 0123.2	12.66%	0.28%
14 0123.2	12.18%	0.01%
15 0123.2	15.47%	0.01%
16 0123.2	16.64%	0.10%
17 0123.2	17.66%	0.01%
18 0123.2	16.74%	0.05%
19 0123.2	16.03%	0.10%
20 0123.2	10.80%	0.16%
21 0123.2	12.51%	0.11%
22 0123.2	20.76%	0.00%
23 0123.2	17.90%	0.05%
24 0123.2	17.31%	0.15%
25 0123.2	16.81%	0.11%
26 0123.2	19.83%	0.12%

Appendix 3: % carbonate of each sample from shale acidification procedure. % sulfur of each sample from CRS analysis.

Sample #	Fe carb in rock (wt.%)	Fe ox in rock (wt.%)	Fe mag in rock (wt.%)	Fe_{py} in rock (wt.%)	Fe_{PRS} in rock (wt.%)	Fe_T in rock (wt.%)	$Fe_{HR/T}$	$Fe_{py/HR}$
Chuskuna								
1221-01	0.039	0.310	0.112	0.201	0.561	6.73	0.18	0.16
1221-02	0.038	0.279	0.118	0.283	0.525	6.05	0.21	0.23
1221-05	0.045	0.279	0.136	0.095	0.584	6.54	0.17	0.08
1221-07	0.052	0.220	0.131	0.217	0.595	5.98	0.20	0.18
1221-10	0.057	0.371	0.141	0.345	0.562	6.42	0.23	0.23
1221-13	0.061	0.289	0.153	0.309	0.635	6.46	0.22	0.21
1221-16	0.052	0.317	0.129	0.138	0.561	6.28	0.19	0.12
1221-20	0.069	0.199	0.138	0.337	0.682	5.80	0.25	0.24
White Sea								
1 0123.2	0.044	0.237	0.353	0.023		5.23	0.13	0.04
2 0123.2	0.086	0.000		0.088		5.00		
3 0123.2	0.051	0.092	0.211	0.048		5.34	0.08	0.12
4 0123.2	0.055	0.087	0.198	0.028		5.28	0.07	0.08
5 0123.2	0.060	0.103	0.218	0.059		5.09	0.09	0.13
6 0123.2	0.027	0.100	0.096	0.558		4.42	0.18	0.71
7 0123.2	0.026	0.139	0.097	1.174		6.02	0.24	0.82
8 0123.2	0.080	0.454	0.103	1.367		7.07	0.28	0.68
9 0123.2	0.038	0.111	0.158	0.048		5.40	0.07	0.13
10 0123.2	0.035	0.086	0.177	0.023		6.29	0.05	0.07
11 0123.2	0.027	0.063	0.103	0.033		4.14	0.05	0.15
12 0123.2	0.035	0.060	0.101	0.034		4.00	0.06	0.15
13 0123.2	0.032	0.064	0.092	0.312		3.63	0.14	0.62
14 0123.2	0.056	0.048	0.098	0.011		3.86	0.06	0.05
15 0123.2	0.038	0.069	0.182	0.008		4.74	0.06	0.03
16 0123.2	0.031	0.065	0.124	0.145		4.57	0.08	0.40
17 0123.2	0.040	0.068	0.237	0.011		5.25	0.07	0.03
18 0123.2	0.042	0.068	0.195	0.072		5.42	0.07	0.19
19 0123.2	0.061	0.053	0.210	0.120		4.24	0.10	0.27
20 0123.2	0.029	0.000		0.250		3.93		
21 0123.2	0.072	0.374	0.202	0.171		4.44	0.18	0.21
22 0123.2	0.061	0.066	0.240	0.002		5.35	0.07	0.01
23 0123.2	0.061	0.063	0.214	0.080		5.15	0.08	0.19
24 0123.2	0.049	0.120	0.298	0.186		5.70	0.11	0.29
25 0123.2	0.037	0.092	0.205	0.170		4.26	0.12	0.34
26 0123.2	0.035	0.153	0.204	0.168		4.99	0.11	0.30

Appendix 4: Results from iron speciation procedure. Fe carb, ox, mag, and PRS used to calculate Fe_{HR}, which is used to calculate the $Fe_{HR/T}$ and $Fe_{py/HR}$ ratios. Columns in green ($Fe_{HR/T}$, $Fe_{py/HR}$) are plotted in figures 9a and 9b.

Sample #	$\varepsilon^{205}Tl_A$	2SD	Tl_A (ppm)	f_A
Chuskuna				
1221-01	-2.56	0.05	0.10	0.23
1221-02	-2.05	0.54	0.12	0.29
1221-05	-2.25	0.42	0.09	0.22
1221-07	-1.01	0.13	0.12	0.31
1221-10	-1.78	0.12	0.09	0.25
1221-13	-2.81	0.02	0.08	0.20
1221-16	-2.83	0.37	0.07	0.17
1221-20	-3.04	0.07	0.11	0.29

Appendix 5: Thallium isotope data reported as $\varepsilon^{205}Tl_A$, with two standard deviations (2SD). 2SD was calculated as reproducibility of the standard. Tl concentration is reported as Tl_A. The subscript "A" attached to the isotopic compositions and concentration data stands for "authigenic" (pyrite-bound Tl). f_A is the fraction of authigenic Tl.

I pledge on my honor that I have not given or received any unauthorized assistance or plagiarize on this assignment